Frontiers in Bioscience Landmark

Front. Biosci. (Landmark Ed) **2026**; 31(3): 47751
https://doi.org/10.31083/FBL47751

Original Research

High-Intensity Interval Training Outperforms Moderate-Intensity Exercise in Hyperlipidemic *ApoE*$^{-/-}$ Mice: A Molecular and Histological Comparison

Chengsi Qian[1], Zuowei Pei[2], Zhou Yang[3], Min Sun[3], Ya Zhang[3], Hongyang Liu[3,*], Yan Sun[1,*]

[1]Department of Cardiology, Zhejiang Province Rongjun Hospital, 314000 Jiaxing, Zhejiang, China
[2]Department of Cardiology, Affiliated Central Hospital of Dalian University of Technology, 116033 Dalian, Liaoning, China
[3]Department of Heart Intensive Care Unit, The First Affiliated Hospital of Dalian Medical University, 116011 Dalian, Liaoning, China
*Correspondence: liuhongyang@firsthosp-dmu.com (Hongyang Liu); 1579938913@qq.com (Yan Sun)
Academic Editor: Ioanna-Katerina Aggeli
Submitted: 28 October 2025 Revised: 3 February 2026 Accepted: 28 February 2026 Published: 20 March 2026

Abstract

Background: Hyperlipidemia is highly prevalent worldwide and can affect cardiac pathophysiology. This study aimed to compare the effects of high-intensity interval training (HIIT) and moderate-intensity continuous training (MICT) on the molecular mechanisms of myocardial stress and pathological remodeling in non-obese apolipoprotein E knockout (*ApoE*$^{-/-}$) mice with hypercholesterolemia. **Methods**: Thirty-five 8-week-old male *ApoE*$^{-/-}$ mice were randomly assigned to four groups as follows: control (normal diet); HFD (high-fat diet); HFD+MICT (60% maximal running speed); and HFD+HIIT (85% maximal running speed). After a 12-week intervention, serum levels of blood lipids and B-type natriuretic peptide (BNP) as well as pathological changes in the myocardial tissue (hematoxylin and eosin staining and Masson's trichrome staining) were detected. Protein expression analyses of lipid metabolism markers (CD36, CD68 (Cluster of Differentiation 36/68), lectin-type oxidized low-density lipoprotein receptor 1 and peroxisome proliferator-activated receptor-gamma), antioxidant regulators (sirtuin 1/3 [SIRT1/3], nuclear factor erythroid 2-related factor 2 [NRF2], and superoxide dismutase 2 [SOD2]), inflammatory cytokines (interleukin [IL]-6 and IL-18), and fibrosis-related proteins (transforming growth factor-beta 1 [TGF-β1], collagen I/III) was performed using immunohistochemistry and western blotting. **Results**: The HFD condition increased serum total cholesterol (TC) and triglyceride (TG) levels, but did not increase body weight, consistent with a lean hyperlipidemia model. Compared with the MICT condition, the HIIT condition demonstrated superior efficacy in reducing HFD-induced TC, TG and BNP levels ($p < 0.05$). Histologically, HIIT reduced myocardial fibrosis and inflammation. HIIT downregulated lipid transporters CD36/CD68, upregulate the antioxidant SIRT1/3-NRF2-SOD2 axis, inhibit pro-inflammatory factors IL-1β, IL-6, and IL-18, and reduce the deposition of fibrotic TGF-β1 and collagen I and III ($p < 0.05$). **Conclusion**: In a non-obese, hypercholesterolemic *ApoE*$^{-/-}$ model, HIIT elicited more favorable molecular signatures than MICT for ameliorating myocardial stress and pathological remodeling in terms of lipid deposition, oxidative stress, inflammation and fibrosis pathways.

Keywords: hyperlipidemia; *ApoE*$^{-/-}$ mice; myocardial stress; high-intensity interval training; moderate-intensity continuous training; lipid metabolism; oxidative stress

1. Introduction

Hyperlipidemia is characterized by abnormally high levels of lipids or lipoproteins in the blood due to abnormal fat metabolism or function, caused by obesity and hereditary disorders such as familial hypercholesterolemia (FH) or metabolic syndrome [1,2]. Patients with hyperlipidemia are approximately twice as likely to develop cardiovascular disease (CVD) than healthy individuals [3]. Studies have demonstrated that hyperlipidemia can lead to vascular atherosclerosis, and cardiac fat accumulation and affect cardiac function and electrophysiological activity [3–5]. Elevated total cholesterol (TC) and free fatty acids levels trigger systemic oxidative stress and proinflammatory milieu [6,7]. Cardiomyocytes reportedly take up oxidized low-density lipoprotein (LDL) through CD36 and lectin-type oxidized low-density lipoprotein receptor 1 (LOX-1), further activating the nuclear factor-kappa B (NF-κB) signaling pathway and promoting inflammation and fibrosis. Inflammation is a major predisposing factor for CVD [7]. In hypercholesterolemia, macrophage infiltration ($CD68^+$) and inflammasome upregulation (interleukin [IL]-1β/IL-18) accelerate plaque instability [8]. Mast cell degranulation releases profibrotic mediators that activate the transforming growth factor-beta (TGF-β)/mothers against decapentaplegic homolog 3 (SMAD3) signaling, promoting collagen I/III deposition and diastolic dysfunction [9]. Hypercholesterolemia significantly decreases the expression of cardiac autophagy markers but increases the levels of cleaved caspase-3, a marker of cardiac apoptosis [10,11]. These perturbations ultimately lead to mitochondrial dysfunction, which is target by deacetylases (sirtuin, SIRT1

and 3 [SIRT1/3]) and the nuclear factor erythroid 2-related factor 2 (NRF2) antioxidant pathway [12].

Exercise training is a critical non-pharmacological intervention for metabolic and CVD. Moderate-intensity continuous training (MICT) improves insulin sensitivity, while high-intensity interval training (HIIT) preferentially enhances mitochondrial biogenesis and oxidative capacity. Structured aerobic exercise reduces the incidence of metabolic and CVD by 30–40% [13]. Exercise exerts cardioprotective effects via antiapoptotic, antifibrotic, and antioxidant mechanisms, mediated by SIRT1/3-NRF2 regulation and mitochondrial quality control [9,13–16]. Exercise reportedly modulates inflammation and lipid metabolism through intensity-dependent regulation of CD36-mediated fatty acid uptake and peroxisome proliferator-activated receptor-gamma (PPAR-γ) transcriptional activity [17]. The pro-inflammatory cytokine IL-6 has been reported to be the strongest predictor of comorbidity and prognosis in patients with chronic kidney disease (CKD), and exercise training reduces IL-6 via *SIRT3*-dependent deacetylation of NF-κB [18]. Regular exercise positively impacts CVD progression by increasing antioxidant capacity via upregulating SOD2 and NRF2 and reducing hyperlipidemia-induced oxidative imbalance [9,14]. Physical activity increases SOD2 expression while reducing malondialdehyde (MDA) levels, reflecting decreased lipid peroxidation, whereas physical activity increases antioxidant enzymes (SOD2) expression while ameliorating oxidative damage-induced cardiac MDA levels [19]. Although HIIT is superior for metabolic syndrome [13,15,16], its effectiveness in non-obese and high-cholesterol conditions remains unknown, and whether the myocardial protective effect of exercise in patients with hyperlipidemia is intensity dependent remains unclear.

This study compared the molecular adaptations between HIIT and MICT in a hypercholesterolemic apolipoprotein E knockout (*ApoE*$^{-/-}$) model by focusing on lipid transport, redox homeostasis, and inflammatory-fibrotic signaling.

2. Materials and Methods

2.1 Experimental Animals

Thirty-five 8-week-old male *ApoE*$^{-/-}$ mice were procured from the Beijing Weitong Lihua Experimental Animal Company Beijing Biotechnology Co., Ltd. (Beijing, China) and randomly allocated into four groups. The groups were defined as follows: Control (n = 7), which received a standard diet (10% calories from fat); HFD (n = 9), which received a high-fat diet (35% fat calories, 1.5% cholesterol); HFD+MICT (n = 10), which received a high-fat diet along with moderate-intensity continuous exercise (60% maximal speed); HFD+HIIT (n = 9), which received a high-fat diet along with high-intensity intermittent exercise (9 × 1.5-min sprints at 85% maximal speed with 1-min rest intervals). The HFD contained 83.5% basal diet, 15% lard, and 1.5% cholesterol (Beijing Biotechnology Co., Ltd. (Beijing, China)), yielding approximately 3.94 kcal/g of energy with 35% calories from fat. This formulation mimics the lean hypercholesterolemic phenotype but not diet-induced obesity. The mice were housed in a controlled environment with a temperature maintained between 24–26 °C, humidity at 40–60%, and exposure to a 12-hour light/dark cycle. Each mouse was provided free access to both food and tap water. At the termination of the study, the mice were euthanized by exsanguination under deep anesthesia. Anesthesia was induced and maintained with 1.5% isoflurane (delivered via nose-cone, flow adjusted by weight). Adequate anesthetic depth was confirmed by monitoring respiratory rate, heart rate, and pedal reflexes before proceeding with carotid artery exsanguination. Blood samples were collected from the carotid artery, centrifuged (3000 rpm, 15 min, 4 °C), and stored in serum tubes at –80 °C until analysis. Cardiac tissues were fixed in 10% formalin for subsequent histological evaluation and embedded in paraffin. The remaining cardiac tissue was rapidly frozen in liquid nitrogen for subsequent western blot analysis. All animal procedures adhered to the guidelines stipulated in the "Guide for the Care and Use of Laboratory Animals" and were approved by the Animal Ethics Committee of Affiliated Central Hospital of Dalian University of Technology (approval No. [2023-057-55]). This approval covered a series of related studies investigating exercise interventions in hyperlipidemic *ApoE*$^{-/-}$ mice, including the present work and subsequent mechanistic studies [15].

2.2 Exercise Training Regimen

To determine the maximum running speed, *ApoE*$^{-/-}$ mice in the exercise group underwent a running test on an XR-PT-10B treadmill (Shanghai XinRuan Information Technology Co., Ltd., Shanghai, China). The test commenced at a speed of 10 m/min with an incline of 0° for 20 min, and the speed was gradually increased by 4 m/min until exhaustion was reached. The mice were considered exhausted if they remained stationary on the grid for 3 s or exhibited no movement in response to gentle nudges with a soft brush. The maximum velocity achieved during exercise was defined as maximum running speed (Vmax). All exercise groups underwent a 5-minute warm-up at 40% Vmax before formal training. For the HFD+HIIT group, the exercise regimen involved nine sets of higher-intensity treadmill exercises at 85% Vmax, each lasting 1.5 min, with a 1-min recovery interval at 40% Vmax between each sprint set, totaling 21.5 min per session. No adverse events (injury or death) occurred during the training, confirming the safety of the intensity protocol for this genotype. Conversely, the HFD+MICT group participated in continuous endurance training, maintaining a speed equivalent to 60% Vmax until their running distance matched that of the HFD+HIIT group. This design ensured that any observed differences were attributable to the intensity modality rather than the

total work volume. Following formal training, both groups underwent a 5-min recovery period at 40% Vmax. This exercise routine was repeated five times per week for 12 weeks.

2.3 Serum Measurements

Serum lipid (TC and triglyceride [TG]) and B-type natriuretic peptide (BNP) levels were quantified using a commercial assay kit, following the protocols outlined by the manufacturer (Nanjing Jiancheng Bioengineering Institute, Nanjing, China).

2.4 Histological Staining

The procured hearts were fixed in 10% neutral-buffered formalin for 24 h, then dehydrated in graded ethanol (75%, 85%, 90%, and 100%, each for 5 min each), and embedded in paraffin. Sections (4 µm) were cut and mounted on glass slides coated with poly-L-lysine. To prepare the sections for analysis, deparaffinization was achieved by immersion in xylene, with three changes of xylene (5 min each). Rehydration was then performed using reduced concentrations of alcohol (100 to 75% for 5 min each). Hematoxylin and eosin (HE) staining was performed according to standard protocols. Masson's trichrome staining was used to visualize the collagen deposition (blue) and myocardial architecture (red) to assess interstitial fibrosis. Imaging was conducted using an upright light microscope (Murzider, Beijing, China) at 200× magnification (objective 20×, numerical aperture 0.45). Scale bars = 20 µm.

2.5 Immunohistochemistry

Heart tissue sections were fixed in 10% formalin, dehydrated using an ethanol series, and embedded in paraffin for a histological evaluation. After deparaffinization and antigen retrieval (citrate buffer, pH 6.0, 95 °C, 20 min), the sections were blocked with 3% H_2O_2 (15 min) and 5% bovine serum albumin (BSA), then incubated overnight with primary antibodies at 4 °C (all from Proteintech, Wuhan, China). The dilutions were as follows: rabbit anti-CD36 (1:600, Cat# 32371-1-AP), rabbit anti-CD68 (1:500, Cat# 30929-1-AP), rabbit anti-PPAR-γ (1:400, Cat# 16643-1-AP), rabbit anti-LOX-1 (1:200, Cat# 11837-1-AP), rabbit anti-interleukin (IL)-1β (1:100, Cat# 26048-1-AP), rabbit anti-IL-6 (1:100, Cat# 21865-1-AP), rabbit anti-IL-10 (1:100, Cat# 15102-1-AP), rabbit anti-IL-18 (1:100, Cat# 10663-1-AP), rabbit anti-NRF2 (1:200, Cat# 16396-1-AP), rabbit anti-SIRT1 (1:200, Cat# 13161-1-AP), rabbit anti-SIRT3 (1:200, Cat# 10099-1-AP), rabbit anti-SOD2 (1:200, Cat# 24127-1-AP), rabbit anti-TGF-β (1:500, Cat# 26155-1-AP), rabbit anti-SMAD3 (1:200, Cat# 30130-1-AP), rabbit anti-Collagen I (1:500, Cat# 14695-1-AP), and rabbit anti-Collagen III (1:1000, Cat# 22734-1-AP). Subsequently, the sections were incubated for 30 min at room temperature with goat anti-rabbit Horseradish Peroxidase (HRP) secondary antibody (Anti-rabbit Universal Immunohistochemical Detection Kit; Cat# PK10006; Proteintech Group, Inc., Wuhan, China). All sections were examined meticulously using an upright light microscope (Nikon ECLIPSE Ti-U, Nikon Corporation, Tokyo, Japan) for a precise and detailed analysis. Positive cells were quantified as the percentage of total nucleated cells in five random high-power fields (200× magnification) per section.

2.6 Western Blotting

Total protein was extracted using Radio Immunoprecipitation Assay (RIPA) buffer (P0013B; Beyotime Biotechnology, Shanghai, China) supplemented with protease/phosphatase inhibitors. The protein concentration was determined using a bicinchoninic assay (Beyotime Biotechnology, Shanghai, China) with bovine serum albumin (BSA) standards and transferred to polyvinylidene fluoride membranes (Immobilon, MilliporeSigma, Billerica, MA, USA). After being blocked with 5% milk/Tris-buffered saline containing 0.1% Tween-20 at room temperature for 1 hour, the membranes were incubated overnight at 4 °C with primary antibodies (all from Proteintech, Wuhan, China) at the following dilutions: rabbit anti-CD36 (Cat# 32371-1-AP), anti-CD68 (Cat# 30329-1-AP), anti-PPAR-γ (Cat# 16643-1-AP), anti-LOX-1 (Cat# 11837-1-AP), anti-SIRT1 (Cat# 13161-1-AP) and anti-SOD2 (Cat# 24127-1-AP) at 1:1000; rabbit anti-SIRT3 (Cat# 10099-1-AP) and anti-NRF2 (Cat# 16396-1-AP) at 1:2000; rabbit anti-β-actin (Cat# 20536-1-AP) at 1:10,000. After being thoroughly washed, the membranes were incubated with the appropriate secondary antibody (anti-rabbit IgG, 1:5000) for 1 h. Bands were quantified using ImageJ software (Version 1.43u, National Institutes of Health, Bethesda, MD, USA), with β-actin serving as the internal control. The protein levels were expressed as protein/β-actin ratios to ensure an accurate and comparative analysis.

2.7 Statistical Analysis

All data are presented as the mean ± standard error of the mean (mean ± SEM). The statistical analyses were performed using GraphPad Prism v9.0 (GraphPad Software, Inc., San Diego, CA, USA). Intergroup differences were assessed using one-way analysis of variance followed by Tukey's post hoc test ($*p < 0.05$, $**p < 0.01$). All histological results were quantified using Image J software by a color threshold analysis of three random areas per section.

3. Results

3.1 Determination of Body Weight, Lipid Levels and BNP Levels

To investigate the effects of different exercise intensities on hyperlipidemia, we established a hyperlipidemia model using a high-cholesterol diet that exhibited a lean hyperlipidemic phenotype. Serological findings indicated notably higher TC and TG in the HFD group, but no significant increase in total body weight or heart weight (Fig. 1),

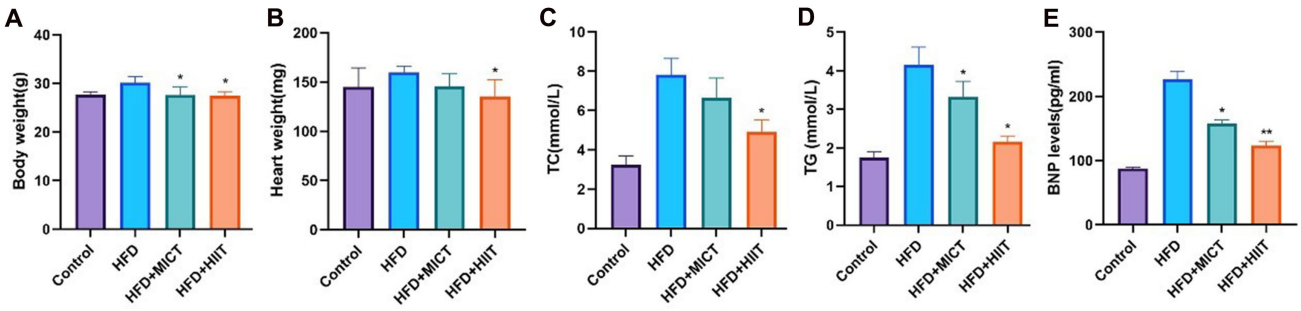

Fig. 1. Effects of high-intensity interval training (HIIT) on body weight, blood lipids levels and B-type natriuretic peptide (BNP) levels in mice. (A) Body weight. (B) Heart weight. (C) Total cholesterol (TC). (D) Triglyceride (TG). (E) BNP. *$p < 0.05$ versus high-fat diet (HFD); **$p < 0.01$ versus HFD. The data are expressed as mean ± SEM, n = 5. MICT, moderate-intensity continuous training.

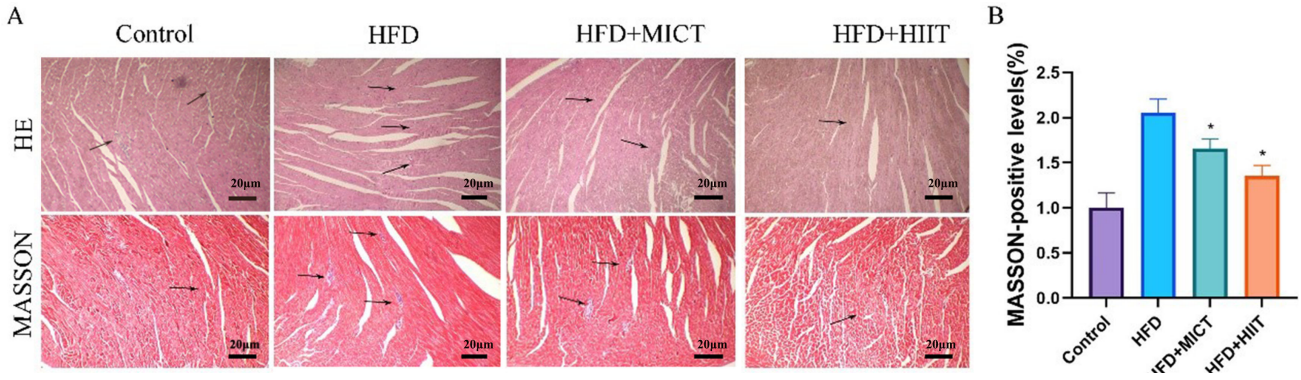

Fig. 2. Histological analysis (hematoxylin and eosin [HE] and Masson's trichrome staining) of the hearts of HFD-fed apolipoprotein E knockout (*ApoE*$^{-/-}$) mice subjected to HIIT. (A) HE-stained tissue showing inflammatory infiltration and microvesicular steatosis in the HFD group. Masson-stained tissue reflecting collagen deposition (blue) and myocardial architecture. 200× magnification, Scale bar = 20 μm. The arrows indicate areas with positively stained cells. (B) Quantitative analysis of areas with positively stained cells. n = 3 per group. *$p < 0.05$ versus HFD.

confirming the successful establishment of the familial hypercholesterolemic mouse model in which cardiac damage precedes systemic obesity. This allowed us to isolate direct myocardial lipotoxicity from the confounding hyperlipidemic effects. In contrast, the HIIT+HFD group exhibited significantly reduced TC and TG levels ($p < 0.05$, Fig. 1), suggesting the efficacy of HIIT at effectively lowering these lipid parameters in the mice. Owing to the limitations of the experimental conditions, echocardiography was not performed to evaluate cardiac function, and BNP was selected as a surrogate index to evaluate cardiac wall stress and hemodynamic load. We further assessed the BNP levels to ascertain their potential protective effects against hyperlipidemia-induced myocardial stress at different exercise intensities. As demonstrated in Fig. 1, HFD increased serum BNP levels 2.4-fold, indicating an increased cardiac load. BNP level was reduced by exercise in both groups, but the HIIT group intervention was more effective ($p < 0.01$). These results suggest that HIIT exerts a significant protective effect against hyperlipidemia-induced myocardial stress.

3.2 HIIT Reduces Myocardial Stress in Hyperlipidemic Mice

The HE results confirmed HFD-induced inflammatory infiltration and microvesicular steatosis in the myocardial tissue. MICT improved these lesions moderately, whereas HIIT significantly reduced them (Fig. 2). Masson's trichrome staining revealed no histological abnormalities in the myocardial structures in the control group. However, the mice in the HFD group showed significant myocardial interstitial fibrosis (blue). The exercise interventions reduced fibrosis, with a modest effect of MICT and a more dramatic effect of HIIT.

3.3 HIIT Reduces Lipid Deposition in HFD-Fed ApoE$^{-/-}$ Mice

These lipid deposition markers collectively capture the full spectrum of lipid handling ranging, from cellular uptake (CD36) and oxidized LDL recognition (LOX-1) to storage regulation (PPAR-γ) and inflammatory responses (CD68), and their dysregulation leads to myocardial lipotoxicity. Our observations indicated substantially elevated CD36, CD68, PPAR-γ, and LOX-1 levels in HFD versus

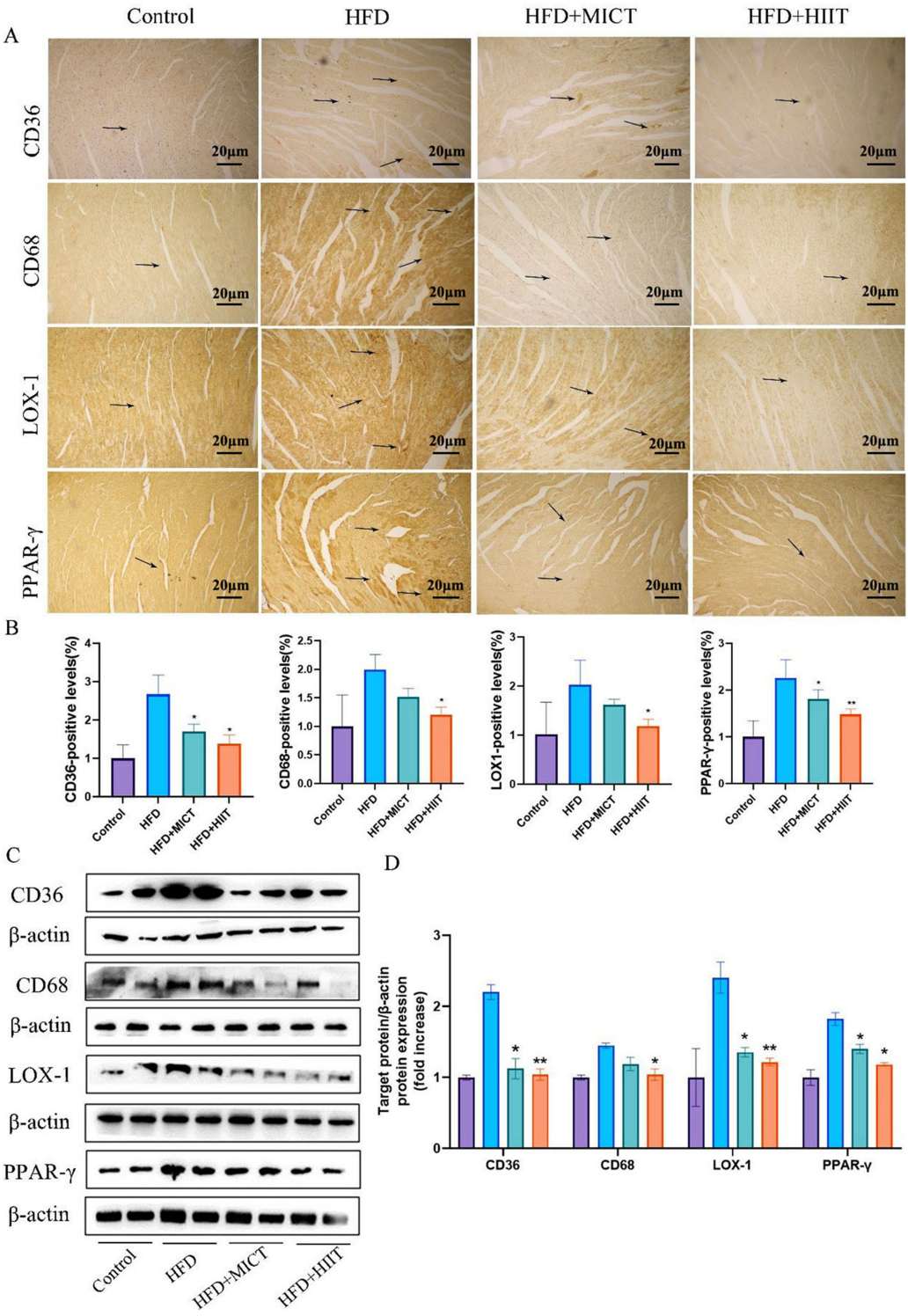

Fig. 3. HIIT reduced lipid metabolism-related protein expression in HFD-fed *ApoE*$^{-/-}$ mice. (A) Immunohistochemical staining of CD36, CD68 (Cluster of Differentiation 36/38), lectin-type oxidized low-density lipoprotein receptor 1 (LOX-1), and peroxisome proliferator-activated receptor-gamma (PPAR-γ). The arrows indicate positively stained cells (brown 3,3′-Diaminobenzidine (DAB) precipitate indicates positivity). 200× magnification; Scale bar = 20 μm. (B) Bar graph showing quantification of immunohistochemical (IHC) positive cell percentage. (C) Western blotting analysis of CD36, CD68, LOX-1 and PPAR-γ protein levels in mice. (D) Bar graph quantifing the lipid metabolism protein. Data are shown as the mean ± SEM; n = 3 per group; *$p < 0.05$ versus HFD, **$p < 0.01$ versus HFD.

control group mice, but HIIT reversed these elevations (all $p < 0.05$ vs. HFD), while MICT showed partial effects (Fig. 3A,B). Changes in protein expression corroborated the immunohistochemical (IHC) data (Fig. 3C,D).

3.4 HIIT is Associated With Reduced Myocardial Oxidative Stress in HFD Mice

Hyperlipidemia is associated with increased reactive oxygen species (ROS) production; therefore, here we examined the effects of different exercise on oxidative stress markers and antioxidants in mice. These markers collectively reflect the mitochondrial antioxidant defense axis, spanning upstream regulators (SIRT1/3), transcriptional activators (NRF2), and the key effector enzyme (SOD2). Our findings revealed a notable reduction in SIRT1, SIRT3, NRF2, and SOD2 levels in HFD mice versus control mice. However, HIIT attenuated the reduction in SIRT1, SIRT3, NRF2, and SOD2 levels observed in the HFD group, as shown in the HIIT+HFD group (Fig. 4).

3.5 HIIT Ameliorates HFD-Induced Inflammation in Mice

IHC was performed to detect the expressions of the HFD-induced inflammation-related factors. We observed increases in IL-1β, IL-6, and IL-18 levels in HFD-induced myocardial stress, but lower IL-10 levels in HFD mice versus control mice (Fig. 5A). While some studies demonstrated that exercise increases IL-10 levels, our finding of reduced IL-10 levels in the exercised groups may reflect intensity-dependent effects or negative feedback from reduced inflammatory stimuli. However, this finding warrants further investigation in future studies. HIIT effectively reduced this elevation. These findings provide compelling evidence of the protective role of HIIT against HFD-induced inflammatory damage (Fig. 5B).

3.6 HIIT Reduces Fibrosis in Mice

Markers such as TGF-β, an upstream cytokine; SMAD3, an intracellular transduction factor; and collagen I/III, the major structural proteins deposited during fibrosis, represent the core of the myocardial fibrosis pathway. The expression levels of SMAD3 and TGF-β were increased in HFD mice. HIIT reversed both effects ($p < 0.01$), whereas MICT partially reduced TGF-β ($p < 0.05$) but not SMAD3 levels (Fig. 6A). Collagen I (fibrotic) was more responsive to HIIT than collagen III (developmental), suggesting that HIIT preferentially reduces pathological fibrosis (Fig. 6B).

4. Discussion

This study used a hypercholesterolemic *ApoE*$^{-/-}$ model without obesity, in which cardiovascular risk is independent of obesity-related factors. Our systematic comparison of HIIT and MICT revealing that HIIT elicits superior signatures, including the downregulation of lipid transporters, upregulation of the SIRT3-NRF2 antioxidant axis, reduction expression of pro-inflammatory cytokines and fibrotic signaling. These intensity-dependent effects are correlated and the requirement for functional validation and causal mechanistic experiments are major limitation (Fig. 7).

Interestingly, Geng *et al.* [20] proposed that excessive exercise paradoxically exacerbates cardiac lipotoxicity via lipid redistribution under high-fat, high-calorie dietary conditions. However, Li *et al.* [21] proposed that compared with MICT, HIIT can comprehensively improve cardiac function and has greater potential to prevent cardiac aging in aged mice. Our research group previously demonstrated that swimming exercise ameliorated hyperlipidemia-induced cardiac injury through anti-inflammatory and antioxidant mechanisms. However, the study did not distinguish between exercise intensities [9]. Hyperlipidemia, a primary CVD risk factor, shows undefined exercise intensity responses in hypercholesterolemic *ApoE*$^{-/-}$ models [9,15]. In this study, a hypercholesterolemic *ApoE*$^{-/-}$ model was successfully established using a dietary formula with 35% fat and 1.5% cholesterol. This model can reproduce myocardial stress caused by hypercholesterolemia without inducing obesity, similar to the clinicopathological features of FH [5,9]. This preliminary study compared HIIT and MICT to identify the optimal exercise protocol for subsequent mechanistic work [15]. In this study, we compared the abilities of HIIT and MICT to reduce hypercholesterolemia-induced myocardial stress within an *ApoE*$^{-/-}$ model without obesity or advanced age. HIIT showed superior protective effects against various aspects of lipid metabolism, oxidative stress, inflammation, and fibrosis cascades, thereby extending previous observations that did not directly compare these exercise modalities. The advantages of HIIT for metabolic diseases were previously reported. Our contribution is the parallel assessment of multiple molecular pathways in an obesity-free mouse model that provided insight into the protective effects of different exercise intensities against hyperlipidemic myocardial stress.

CD36 is a membrane fatty acid transporter whose myocardial upregulation contributes to lipotoxicity [7,17]. CD68 is a marker of macrophage infiltration that reflects inflammatory cell recruitment [8,22]. LOX-1 mediates the uptake of atherogenic lipoproteins, thereby triggering oxidative stress [7,22,23]. PPAR-γ regulates lipid storage but can exacerbate cardiac lipotoxicity when overexpressed [17]. CD36 and LOX-1 expressions were increased in visceral mature adipocytes of obese patients versus non-obese controls [22,24]. Our findings suggest that HIIT has a stronger lipid-lowering effect than MICT. In FH-like models (unlike metabolic syndrome), PPAR-γ upregulation is maladaptive; the HIIT-induced suppression likely dampens excessive lipid storage. The CD68 reduction after HIIT suggests anti-inflammatory polarization, whereas CD36 downregulation may limit lipotoxicity at the potential cost of impaired fatty acid oxidation—a trade-off re-

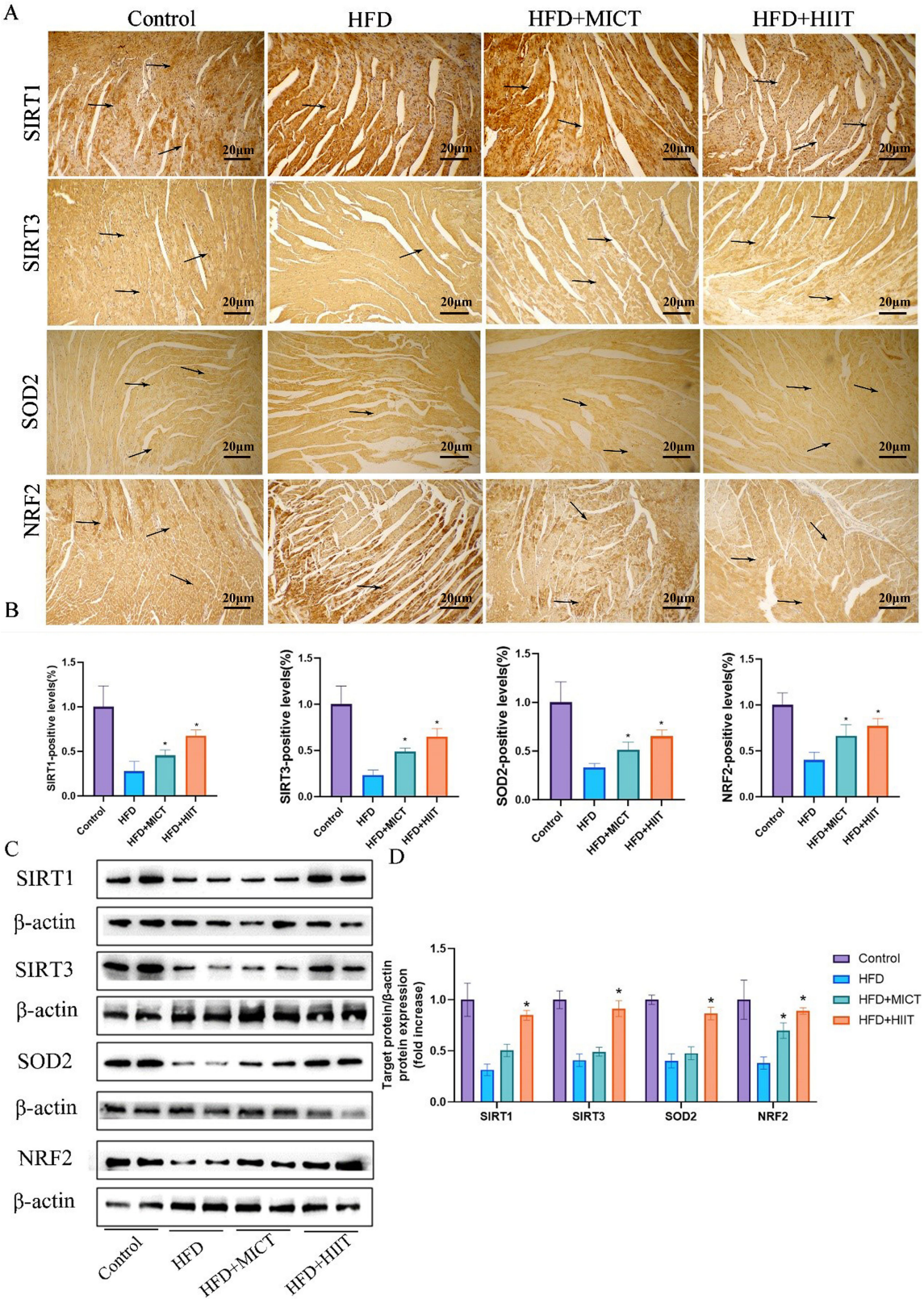

Fig. 4. HIIT reduces antioxidant protein expression in HFD-fed *ApoE*$^{-/-}$ mice. (A) Immunohistochemical staining of sirtuin 1 (SIRT1), sirtuin 3 (SIRT3), superoxide dismutase 2 (SOD2), and nuclear factor erythroid 2-related factor 2 (NRF2). The arrows indicate positively stained cells. Scale bar = 20 μm at 200×magnification. (B) Bar graph quantifying IHC positive cell percentage (SIRT1, SIRT3, SOD2, and NRF2). Data are shown as the mean ± SEM; n = 3 per group; *$p < 0.05$ versus HFD. (C) Western blot analysis of SIRT1, SIRT3, SOD2, and NRF2 in mice. (D) Bar graph showing the quantification of antioxidant protein expression. Data are shown as the mean ± SEM; n = 3 per group; *$p < 0.05$ versus HFD.

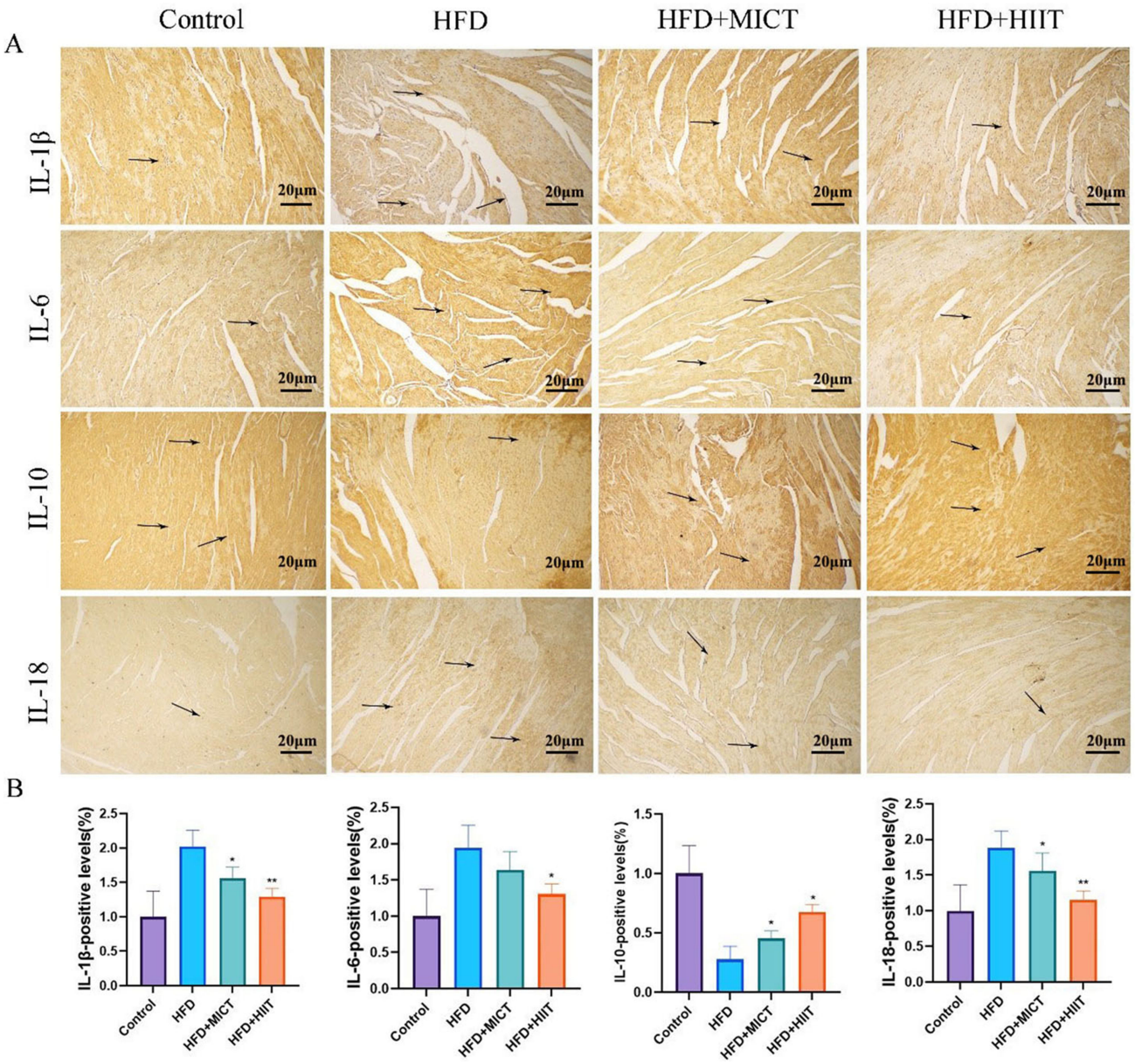

Fig. 5. HIIT reduces inflammatory marker expression in HFD-fed *ApoE*$^{-/-}$ mice. (A) Immunohistochemical staining for interleukin (IL)-1β, IL-6, IL-10, and IL-18. The arrows indicate positively stained cells. Scale bar = 20 μm at 200× magnification. (B) Bar graph quantifying IHC-positive cell percentages. Data are shown as the mean ± SEM; n = 3 per group; *$p < 0.05$ versus HFD group. **$p < 0.01$ versus HFD.

quiring metabolic flux studies. LOX-1 suppression is particularly protective in FH where oxidated LDL is abundant. Our 1.5% cholesterol dose, although supraphysiological, is necessary for rapid atherogenesis in *ApoE*$^{-/-}$ mice, a limitation when extrapolating to human patients with FH.

Oxidative stress is the major manifestation of peripheral atherosclerosis. SIRT1/3 is a Nicotinamide Adenine Dinucleotide (NAD^+)-dependent deacetylases that governs mitochondrial function and antioxidant responses [15,25]. SIRT1 orchestrates lipid and glucose metabolism by deacetylating target proteins, thus assuming a crucial regulatory function in cellular stress resistance, energy metabolism, and tumorigenesis [25,26]. NRF2 is a master transcriptional activator of cellular antioxidant defense because it regulates over 200 cytoprotective genes in response to oxidative stress [27,28]. SOD2 is a mitochondrial antioxidant enzyme that mediates myocardial protection via NRF2 [28]. SIRT3, a NAD^+-dependent deacetylase primarily situated within the mitochondria, governs numerous mitochondrial proteins through post-translational modifications [15,26]. SIRT3 activates SOD2 via deacetylation, thereby enhancing intracellular ROS scavenging activity [29]. Exercise significantly reduces oxidative stress caused by hyperlipidemia. In addition, HIIT was associated

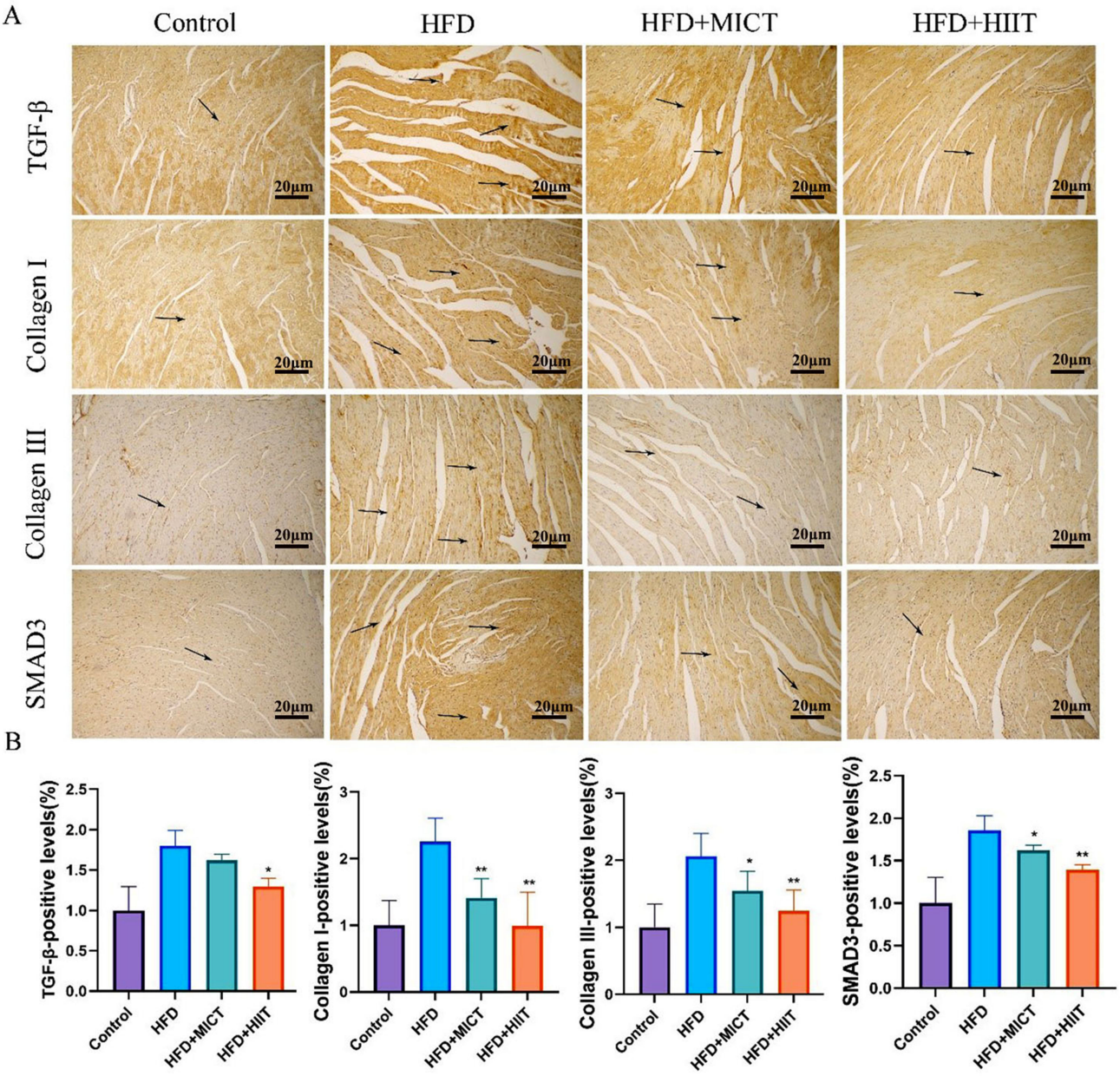

Fig. 6. HIIT reduces the expression of fibrotic markers in HFD-fed *ApoE*$^{-/-}$ mice. (A) Immunohistochemical staining of collagen I, collagen III, mothers against decapentaplegic homolog 3 (SMAD3), and transforming growth factor-beta (TGF-β) in the cardiac tissues. The arrows indicate positively stained cells. (B) Bar graph quantifying the IHC positive cell percentage (collagen I, collagen III, SMAD3, and TGF-β); Scale bar = 20 μm at 200× magnification. The data are shown as the mean ± SEM; n = 3 per group; *$p < 0.05$ versus HFD; **$p < 0.01$ versus HFD.

with greater attenuation of hyperlipidemia-induced cardiac oxidative stress damage compared to MICT group.

The chemokine system plays a key role in the pathophysiology of cardiometabolic diseases. Myocardial IL-1β, IL-6, IL-18, and IL-10 are established inflammatory mediators driving metabolic disease pathogenesis [30,31]. LDL cholesterol stimulates inflammasome activation, precipitating the synthesis of IL-1β and IL-18, subsequently hastening atherosclerosis progression [22–24]. Similarly, HIIT decreased the production of IL-related factors by peritoneal macrophages [32]. While some studies have shown that exercise increases IL-10 levels, our finding of reduced IL-10 levels in the exercise groups may reflect intensity-dependent effects or negative feedback from reduced inflammatory stimuli. This warrants investigation in future studies.

Hyperlipidemia drives myocardial fibrosis through TGF-β1/Smad3-mediated collagen I/III deposition, which ultimately leads to ventricular remodeling and heart failure [9]. The TGF-β1/Smad 3 signaling pathway regulates my-

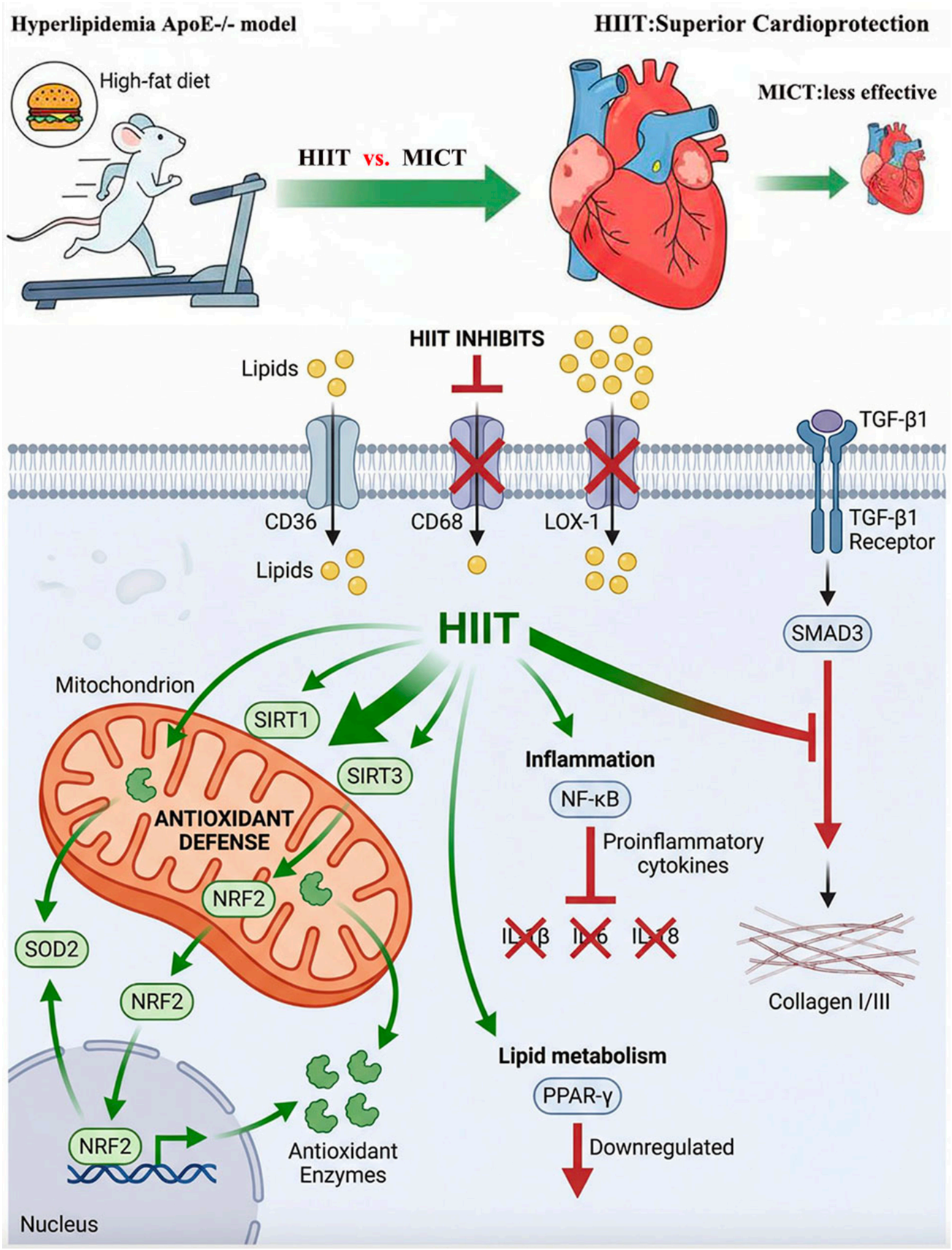

Fig. 7. Proposed molecular mechanism illustrating the superior cardioprotective effects of HIIT versus MICT in hyperlipidemic *ApoE*$^{-/-}$ mice. Created using Gemini, Nanobanana, and Adobe Photoshop (https://gmn.hopeai.cc; https://www.nanoai.cn).

ocardial fibrosis, and TGF-β1 promotes the progression of myocardial fibrosis through Smad3 phosphorylation. Consistently, the knockout of both genes in fibroblasts alleviated pressure overstress-induced fibrosis in mice [9,33]. The present study observed that HFD upregulated the entire fibrosis axis: TGF-β, interstitial staining, SMAD3 nuclear translocation, and collagen I/III deposition. HIIT reversed these changes more effectively than MICT, suggesting that the former has a stronger anti-fibrotic effect. This may reflect the dual inhibition of HIIT on upstream lipid toxicity (reduction of CD36/LOX-1) and inflammation (reduction of IL-1β/6/18), and its protective effect on myocardial stress may be based on the disruption of the lipotoxicity-inflammation-fibrosis cascade.

Study Limitations

Although BNP can be used as a valid surrogate for cardiac load [34], the lack of echocardiographic assessments is a major limitation. Therefore, our conclusions are limited to molecular and histological correlates of myocardial stress rather than functional outcomes. Due to limited sample resources, comprehensive transcriptional validation was not performed. All mechanistic conclusions in this study are hypothesis-generating rather than definitive. This study only compared different exercise intensities at the molecular level, and in-depth mechanistic studies are required in the future. Our study cannot explain the general superiority of HIIT in myocardial damage in patients with hypercholesterolemia, especially in those with obesity and metabolic syndrome or in the elderly population.

5. Conclusions

In the non-obese hypercholesterolemic *ApoE*$^{-/-}$ model used in this study, HIIT elicited superior molecular adaptations compared to MICT by upregulating antioxidant defenses, downregulating of lipid deposition, suppressing pro-inflammatory cytokines, and reducing fibrotic signaling. However, these conclusions are limited by the absence of functional cardiac assessment and direct quantification of myocardial lipid content; thus further functional validation of our findings is required (Fig. 7).

Availability of Data and Materials

All data generated and analyzed during this study are included in this published article and its supplementary information files. The datasets analyzed during the current study are available from the corresponding author upon reasonable request.

Author Contributions

Conceptualization, supervision and project administration, HL and YS. Writing-original draft and data analysis, CQ; Animal experiments and sample collection, HL and ZP; Investigation and data curation, ZY and MS; Formal analysis and Methodology, MS and YZ; Funding acquisition, HL and YS. All authors contributed to editorial changes in the manuscript. All authors read and approved the final manuscript. All authors have participated sufficiently in the work and agreed to be accountable for all aspects of the work.

Ethics Approval and Consent to Participate

All animal procedures adhered to the guidelines stipulated in the "Guide for the Care and Use of Laboratory Animals" and were approved by the Animal Ethics Committee of Affiliated Central Hospital of Dalian University of Technology (approval No. [2023-057-55]).

Acknowledgment

Not applicable.

Funding

This research was funded by Jiaxing Key Laboratory of Cardiac Rehabilitation, grant number 2022002.

Conflict of Interest

The authors declare no conflict of interest. Given his role as the Guest Editor, Zuowei Pei had no involvement in the peer-review of this article and has no access to information regarding its peer review. Full responsibility for the editorial process for this article was delegated to Ioanna-Katerina Aggeli.

Declaration of AI and AI-Assisted Technologies in the Writing Process

During the preparation of this work, the author used Gemini and Nanobanana to generate figures and visualizations. The author reviewed and edited the content as needed and takes full responsibility for its accuracy and integrity.

References

[1] Agha AM, Virani SS, Ballantyne CM. Transatlantic guidelines on dyslipidemia and cardiovascular risk: key differences across the pond. Current Opinion in Endocrinology, Diabetes, and Obesity. 2021; 28: 114–121. https://doi.org/10.1097/MED.0000000000000608.

[2] Pirillo A, Norata GD. The burden of hypercholesterolemia and ischemic heart disease in an ageing world. Pharmacological Research. 2023; 193: 106814. https://doi.org/10.1016/j.phrs.2023.106814.

[3] Yao YS, Li TD, Zeng ZH. Mechanisms underlying direct actions of hyperlipidemia on myocardium: an updated review. Lipids in Health and Disease. 2020; 19: 23. https://doi.org/10.1186/s12944-019-1171-8.

[4] van de Woestijne AP, Monajemi H, Kalkhoven E, Visseren FLJ. Adipose tissue dysfunction and hypertriglyceridemia: mechanisms and management. Obesity Reviews: an Official Journal of the International Association for the Study of Obesity. 2011; 12: 829–840. https://doi.org/10.1111/j.1467-789X.2011.00900.x.

[5] Lyons ARM, Stevens CAT, Dharmayat KI, Vallejo-Vaz DAJ, Ray KK. Overview of a collaborative global effort to address the burden of familial hypercholesterolaemia. Indian Heart Jour-

nal. 2024; 76 Suppl 1: S113–S116. https://doi.org/10.1016/j.ihj.2023.11.005.

[6] Ježek P, Jabůrek M, Holendová B, Plecitá-Hlavatá L. Fatty Acid-Stimulated Insulin Secretion vs. Lipotoxicity. Molecules (Basel, Switzerland). 2018; 23: 1483. https://doi.org/10.3390/molecules23061483.

[7] Biswas S, Gao D, Altemus JB, Rekhi UR, Chang E, Febbraio M, *et al*. Circulating CD36 is increased in hyperlipidemic mice: Cellular sources and triggers of release. Free Radical Biology & Medicine. 2021; 168: 180–188. https://doi.org/10.1016/j.freeradbiomed.2021.03.004.

[8] Tan L, Lu J, Zhang C, Meng L, Zhu Q. The proatherosclerotic function of BCAT1 in atherosclerosis development of aged-apolipoprotein E-deficient mice. Biochemical and Biophysical Research Communications. 2022; 631: 93–101. https://doi.org/10.1016/j.bbrc.2022.09.041.

[9] Pei Z, Ji J, Gao Y, Wang H, Wu Y, Yang J, *et al*. Exercise reduces hyperlipidemia-induced cardiac damage in apolipoprotein E-deficient mice via its effects against inflammation and oxidative stress. Scientific Reports. 2023; 13: 9134. https://doi.org/10.1038/s41598-023-36145-w.

[10] Giricz Z, Koncsos G, Rajtík T, Varga ZV, Baranyai T, Csonka C, *et al*. Hypercholesterolemia downregulates autophagy in the rat heart. Lipids in Health and Disease. 2017; 16: 60. https://doi.org/10.1186/s12944-017-0455-0.

[11] Li K, Deng Y, Deng G, Chen P, Wang Y, Wu H, *et al*. High cholesterol induces apoptosis and autophagy through the ROS-activated AKT/FOXO1 pathway in tendon-derived stem cells. Stem Cell Research & Therapy. 2020; 11: 131. https://doi.org/10.1186/s13287-020-01643-5.

[12] Jawaria, Zarlashat Y, Philippovich M, Dósa E. Nicotinamide N-Methyltransferase in Cardiovascular Diseases: Metabolic Regulator and Emerging Therapeutic Target. Biomolecules. 2025; 15: 1281. https://doi.org/10.3390/biom15091281.

[13] Eijsvogels TMH, Molossi S, Lee DC, Emery MS, Thompson PD. Exercise at the Extremes: The Amount of Exercise to Reduce Cardiovascular Events. Journal of the American College of Cardiology. 2016; 67: 316–329. https://doi.org/10.1016/j.jacc.2015.11.034.

[14] Valaei K, Taherkhani S, Arazi H, Suzuki K. Cardiac Oxidative Stress and the Therapeutic Approaches to the Intake of Antioxidant Supplements and Physical Activity. Nutrients. 2021; 13: 3483. https://doi.org/10.3390/nu13103483.

[15] Gao S, Yao W, Yang J, Liu Y, Pei Z. High intensity exercise training inhibits excessive autophagy in the hyperlipidemic myocardium of ApoE$^{-/-}$ mice via the NAD^{+} mediated SIRT1/MFN2 pathway. Molecular Medicine Reports. 2026; 33: 43. https://doi.org/10.3892/mmr.2025.13753.

[16] Khalafi M, Mohebbi H, Symonds ME, Karimi P, Akbari A, Tabari E, *et al*. The Impact of Moderate-Intensity Continuous or High-Intensity Interval Training on Adipogenesis and Browning of Subcutaneous Adipose Tissue in Obese Male Rats. Nutrients. 2020; 12: 925. https://doi.org/10.3390/nu12040925.

[17] Zhang Y, Xu J, Zhou D, Ye T, Zhou P, Liu Z, *et al*. Swimming exercise ameliorates insulin resistance and nonalcoholic fatty liver by negatively regulating PPARγ transcriptional network in mice fed high fat diet. Molecular Medicine (Cambridge, Mass.). 2023; 29: 150. https://doi.org/10.1186/s10020-023-00740-4.

[18] Bal NB, Sadi G, Bostanci A, Kiremitci S, Adanir I, Uludag MO, *et al*. Effect of Regular Exercise and Resveratrol on Hypertension-Induced Cellular Stress Response and Senescence in Renal and Vascular Tissues of Rats. Journal of Cardiovascular Pharmacology. 2025; 86: 463–477. https://doi.org/10.1097/FJC.0000000000001744.

[19] Wang ZZ, Xu HC, Zhou HX, Zhang CK, Li BM, He JH, *et al*. Long-term detraining reverses the improvement of lifelong exercise on skeletal muscle ferroptosis and inflammation in aging rats: fiber-type dependence of the Keap1/Nrf2 pathway. Biogerontology. 2023; 24: 753–769. https://doi.org/10.1007/s10522-023-10042-1.

[20] Geng J, Zhang X, Guo Y, Wen H, Guo D, Liang Q, *et al*. Moderate-intensity interval exercise exacerbates cardiac lipotoxicity in high-fat, high-calories diet-fed mice. Nature Communications. 2025; 16: 613. https://doi.org/10.1038/s41467-025-55917-8.

[21] Li Q, Liu Q, Lin Z, Lin W, Lin Z, Huang F, *et al*. Comparison Between the Effect of Mid-Late-Life High-Intensity Interval Training and Continuous Moderate-Intensity Training in Old Mouse Hearts. The Journals of Gerontology. Series A, Biological Sciences and Medical Sciences. 2025; 80: glaf025. https://doi.org/10.1093/gerona/glaf025.

[22] Santiago-Fernández C, Pérez-Belmonte LM, Millán-Gómez M, Moreno-Santos I, Carrasco-Chinchilla F, Ruiz-Salas A, *et al*. Overexpression of scavenger receptor and infiltration of macrophage in epicardial adipose tissue of patients with ischemic heart disease and diabetes. Journal of Translational Medicine. 2019; 17: 95. https://doi.org/10.1186/s12967-019-1842-2.

[23] Akhmedov A, Sawamura T, Chen CH, Kraler S, Vdovenko D, Lüscher TF. Lectin-like oxidized low-density lipoprotein receptor-1 (LOX-1): a crucial driver of atherosclerotic cardiovascular disease. European Heart Journal. 2021; 42: 1797–1807. https://doi.org/10.1093/eurheartj/ehaa770.

[24] Santiago-Fernández C, Martin-Reyes F, Tome M, Ocaña-Wilhelmi L, Rivas-Becerra J, Tatzber F, *et al*. Oxidized LDL Modify the Human Adipocyte Phenotype to an Insulin Resistant, Proinflamatory and Proapoptotic Profile. Biomolecules. 2020; 10: 534. https://doi.org/10.3390/biom10040534.

[25] Ren BC, Zhang YF, Liu SS, Cheng XJ, Yang X, Cui XG, *et al*. Curcumin alleviates oxidative stress and inhibits apoptosis in diabetic cardiomyopathy via Sirt1-Foxo1 and PI3K-Akt signalling pathways. Journal of Cellular and Molecular Medicine. 2020; 24: 12355–12367. https://doi.org/10.1111/jcmm.15725.

[26] Yaghoobi A, Rezaee M, Hedayati N, Keshavarzmotamed A, Khalilzad MA, Russel R, *et al*. Insight into the cardioprotective effects of melatonin: shining a spotlight on intercellular Sirt signaling communication. Molecular and Cellular Biochemistry. 2025; 480: 799–823. https://doi.org/10.1007/s11010-024-05002-3.

[27] Chen QM. Nrf2 for protection against oxidant generation and mitochondrial damage in cardiac injury. Free Radical Biology & Medicine. 2022; 179: 133–143. https://doi.org/10.1016/j.freeradbiomed.2021.12.001.

[28] Cui C, Song H, Guo Y, Shi J, Geng B, Wang G. The Nrf Family and Its Cardioprotective Potential: Mechanisms, Functions, and Therapeutic Perspectives. Drug Design, Development and Therapy. 2025; 19: 8339–8373. https://doi.org/10.2147/DDDT.S547848.

[29] Cao X, Wu Y, Hong H, Tian XY. Sirtuin 3 Dependent and Independent Effects of NAD^{+} to Suppress Vascular Inflammation and Improve Endothelial Function in Mice. Antioxidants (Basel, Switzerland). 2022; 11: 706. https://doi.org/10.3390/antiox11040706.

[30] Ridker PM, Rane M. Interleukin-6 Signaling and Anti-Interleukin-6 Therapeutics in Cardiovascular Disease. Circulation Research. 2021; 128: 1728–1746. https://doi.org/10.1161/CIRCRESAHA.121.319077.

[31] Sigrist-Flores SC, Ponciano-Gómez A, Pedroza-González A, Gallardo-Ortíz IA, Villalobos-Molina R, Pardo-Vázquez JP, *et al*. Chronic intake of moderate fat-enriched diet induces fatty liver and low-grade inflammation without obesity in rabbits. Chemico-biological Interactions. 2019; 300: 56–62. https://do

i.org/10.1016/j.cbi.2019.01.004.

[32] Feng L, Li G, An J, Liu C, Zhu X, Xu Y, *et al*. Exercise Training Protects Against Heart Failure Via Expansion of Myeloid-Derived Suppressor Cells Through Regulating IL-10/STAT3/S100A9 Pathway. Circulation. Heart Failure. 2022; 15: e008550. https://doi.org/10.1161/CIRCHEARTFAILURE.121.008550.

[33] Khalil H, Kanisicak O, Prasad V, Correll RN, Fu X, Schips T, *et al*. Fibroblast-specific TGF-β-Smad2/3 signaling underlies cardiac fibrosis. The Journal of Clinical Investigation. 2017; 127: 3770–3783. https://doi.org/10.1172/JCI94753.

[34] Bastos JM, Scala N, Perpétuo L, Mele BH, Vitorino R. Integrative bioinformatic analysis of prognostic biomarkers in heart failure: Insights from clinical trials. European Journal of Clinical Investigation. 2025; 55: e70010. https://doi.org/10.1111/eci.70010.